

Association between El Niño and extreme temperatures in southern South America
in CMIP5 models. Part 2: future climate projections

Soledad Collazo^{1*}, Mariana Barrucand^{1,2}, Matilde Rusticucci^{1,2}

¹Departamento de Ciencias de la Atmósfera y los Océanos, Facultad de Ciencias Exactas y Naturales, Universidad de Buenos Aires, Ciudad Universitaria, 1428 Buenos Aires, Argentina (DCAO-FCEN-UBA)

²Consejo Nacional de Investigaciones Científicas y Técnicas, 1425 Buenos Aires, Argentina (CONICET)

Running page title: ENSO and extreme temperatures in CMIP5

*Corresponding author address:

Departamento de Ciencias de la Atmósfera y los Océanos, Facultad de Ciencias Exactas y Naturales, Universidad de Buenos Aires

Intendente Güiraldes 2160, Ciudad Universitaria Pab II, 1428 Buenos Aires, Argentina

Tel/fax: +54 11 52858471

Email: scollazo@at.fcen.uba.ar

ORCID Soledad Collazo: 0000-0001-7785-2998

ORCID Mariana Barrucand: 0000-0001-5385-2491

ORCID Matilde Rusticucci: 0000-0003-2588-6234

Abstract

This study provides an overview of the future projected changes in the probability density function (PDF) and variability of the equatorial Pacific sea surface temperature in the El Niño 3.4 region (SST3.4). Moreover we analyzed how these changes affect the relationship with the extreme temperature events in southern South America under global warming. We used two different emission scenarios for climate change simulations in the Coupled Model Intercomparison Project Phase 5 (CMIP5), RCP4.5 and 8.5, and for two future periods: 2031-2060 and 2071-2100. The Kolmogorov-Smirnov test was applied to compare the PDFs of SST3.4 among the historical and futures periods. We found that PDFs of SST3.4 for both future periods significantly differ from the PDFs in the historical period for both scenarios. Changes in SST3.4 under greenhouse warming will alter the intensity and position of the teleconnection patterns. In particular, we observed that the mean difference of sea level pressure anomalies between El Niño and La Niña would weaken in the future. This result could explain that, in general, no significant correlations and quantileregression slopes at the 90th percentile between SST3.4 and extreme temperature indices in southern South America were projected for both the near and far future. The projections of the models with the best performance in the historical period did not provide much clarity because they display some differences between them but showed us that the individual models simulate changes in the relationships between SST3.4 and extremes temperature according to the period and the scenario.

Keywords:Climate extremes; Global Climate Models; ENSO teleconnections; Projections; Correlations; Quantile regression; Argentina

1. Introduction

El Niño-Southern Oscillation (ENSO) is the most predominant mode of interannual climate variability in the tropical Pacific as well as in remote regions around the world (Yeh et al. 2018). ENSO manifests itself through anomalous sea surface temperatures (SST) in the equatorial Pacific that trigger Rossby wave trains from the tropics to higher latitudes (Karoly 1989). These wave trains traveling across the atmosphere are known as teleconnections. ENSO influences precipitation and surface air temperature over many parts of the globe through atmospheric teleconnections (Ropelewski & Halpert 1987, Halpert & Ropelewski 1992).

ENSO can affect the intensity and occurrence of extreme events such as heatwaves, droughts, and floods (King et al. 2016). In the first part of this work (Collazo et al. 2021), we analyzed ENSO association with four extreme temperature climate indices in southern South America. We showed that warm SST in the El Niño 3.4 region is associated with a higher occurrence of warm extremes of minimum temperature in northern and central Argentina and Chile, southern Brazil, and Uruguay during the winter and spring.

ENSO variability and teleconnections are embedded in climate change, and their response will be largely dependent on two factors: changes in the mean state both in

the tropical Pacific and elsewhere around the globe, and changes in ENSO properties such as its spatial pattern and amplitude (Yeh et al. 2018).

Global Climate Models (GCMs) are a necessary tool to simulate the future climate. Coupled Model Intercomparison Project Phase 5 (CMIP5) provides coordinated simulations of the state-of-the-art of climate system and utilizes a set of emission scenarios based on Representative Concentration Pathways (RCPs) for future projections (Taylor et al. 2012). RCPs are prescribed pathways for greenhouse gases and aerosol concentrations, together with land-use change (van Vuuren et al. 2011). The pathways are characterized by the radiative forcing produced by the end of the 21st century, i.e., the extra heat that the lower atmosphere will retain as a result of additional greenhouse gases.

The diversity and complexity of ENSO remain to be a challenge for the climate modelers (Capotondi et al. 2015). GCMs project large changes in the tropical Pacific mean state in response to global warming; however, the changes in ENSO amplitude are highly model dependent (Yeh & Kirtman 2007, Collins et al. 2010, Bellenger et al. 2014). Nevertheless, there is modeling evidence that ENSO activity will increase in association with an increment vertical oceanic stratification due to global warming (Cai et al. 2015, Wang et al. 2019, Carréric et al. 2020).

Regardless of uncertainties on ENSO projections, climate models suggest that ENSO teleconnections will change due to differences in the mean atmospheric circulation as a result of anthropogenic forcing in the 21st century (Yeh et al. 2018). The climatological mean state of the extratropical atmosphere influences the propagation of tropically forced Rossby waves and their teleconnections (Branstator 1984,

Trenberth et al. 1998 and reference therein). Meehl et al. (1993, 2006) identify a weaker ENSO teleconnection in the mid-latitudes resulting from changes in the mid-latitude mean state in the future climate. However, future changes in ENSO amplitude (Guilyardi et al. 2012, Kim & Yu 2012, Stevenson et al. 2012) and its teleconnections (Sterl et al. 2007) are strongly dependent on the model used, since the signal is usually small compared to the natural variability (Stevenson 2012). Therefore, there are many uncertainties about ENSO future projections in terms of changes in amplitude, variability, and pattern (Collins et al. 2010). Despite the lack of agreement of the climate models, there is a consistently projected strengthening of the atmospheric response to ENSO across the equatorial Pacific (Power et al. 2013, Cai et al. 2014, Perry et al. 2017). Furthermore, chapter 14 of the Fifth Assessment of Intergovernmental Panel on Climate Change (Christensen et al. 2013) concluded that there was high confidence that ENSO will remain the dominant mode of interannual variability with global influences in the 21st century (Collins et al. 2010, Guilyardi et al. 2012, Kim & Yu 2012, Stevenson 2012).

The projections also indicate changes in extreme temperature indices congruent with warmer conditions of both cold and warm extremes, i.e., a constant and significant decrease in cold nights (TN10p) and cold days (TX10p), and an overall significant increase in warm nights and days (TN90p and TX90p, respectively) from the end of the 20th century to the 21st century in all the Representative Concentration Paths (RCP) scenarios (Seneviratne et al. 2012). However, the smallest change in the minimum temperature percentile indices (TN10p and TN90p) is predicted for southern South America (Sillmann et al. 2013b). For both the summer and winter minimum and maximum temperatures, the highest percentiles will increase significantly more than

1 the lowest in almost all the globe, although this asymmetric is most pronounced in the
2 northern hemisphere (Kodra&Ganguly 2014).The future projections by an ensemble of
3 regional climate models in South America show that, during the austral summer,
4 theincrease in the frequency of warm nights is larger than that projected for warm days
5 (López-Franca et al. 2016). The authors suggest that thisbehavior in La Plata Basin is
6 consistent with the cooling effect of cloud cover affecting maximum temperature, while
7 minimum temperature is affected bynighttime greenhouse warming.

8 In order to understand the causes of the extreme events changes, it is necessary to
9 analyze how their main forcings could evolve under climate change conditions. Up
10 today, there has been limited research investigating future changes in extreme
11 temperatures in South America due to changes in ENSO teleconnections. There is still a
12 debate in the scientific community about the future projections of ENSO
13 teleconnections and the role of regional air-sea coupled processes outside the tropics
14 in modulating these ENSO atmospheric teleconnections (Yeh et al. 2018).These
15 uncertainties are due to the fact climate models simulate equatorial cold tongues
16 extending too far westward, which in turn produces biased ENSO precipitation
17 teleconnections (Cai et al. 2009). In addition, biases in other oceanic basins can
18 influence the representation of ENSO strength and timing of atmospheric
19 teleconnections (Taschetto et al. 2020). The complexity and diversity of the
20 teleconnections are because it depends on multiple nonlinear factors (Capotondi et al.
21 2015).

22 The goal of this study is to evaluate the changes projected by two RCPs scenarios,
23 RCP4.5 and RCP8.5, in the variability and distributions of the sea surface temperature

(SST) in the equatorial Pacific as well as changes in the ENSO teleconnection with extreme temperature events in southern South America in the near (2031-2060) and far (2071-2100) future. In order to assess the teleconnections, we estimated the correlations and quantile regressions between SST and four extreme temperature indices globally used.

2. Data and methodology

In order to study changes in the variability and distribution of the sea surface temperature in the equatorial Pacific, we used CMIP5 modeled SST data in El Niño 3.4 region (SST3.4, 5°N – 5°S, 170-120°W) in the historical period (1976-2005), near future (2031-2060), and far future (2071-2100), obtained from KNMI Climate Explorer (<https://climexp.knmi.nl/start.cgi>, access 12/08/2020). As a reference to the historical period, we additionally included the observed SST in the El Niño 3.4 region (SST3.4) of the Hadley Centre Global Sea Ice and Sea Surface Temperature (HadISST) version 1.1 (Rayner et al. 2003).

To represent the ENSO teleconnection in the past and the future, we employed sea-level pressure (SLP) anomalies in the southern hemisphere for the same GCMs in Collazo et al. (2021)(Table S1). The anomalies were estimated for the climatological period 1981-2010. The projected induced changes in extreme temperature events in southern South America (20 –60°S, 75 – 50°W) by the ENSO were explored considering four climate indices used internationally (Table 1), defined by Expert Team on Climate Change Detection and Indices (ETCCDI). These extremes were simulated by CMIP5 models in both near and far future periods. These indices are based on a percentile

threshold, i.e., they describe the exceedance rates above or below a threshold defined as the 10th or 90th percentile derived from the 1961–1990 base period. This data is available on the webpage <http://climate-modelling.canada.ca/climatemodeldata/climindex/climindex.shtml> (Access 12/08/2020).

The RCP4.5 and RCP8.5 climate scenarios were considered to represent moderate and extreme global warming, respectively. The RCP scenarios do not produce discernibly different climate change until mid-century, while long-term climate change by the end of the century is appreciably different across the RCPs (IPCC 2014). This difference motivated the use of two future periods. We used extreme temperature indices from the same CMIP5 GCMs and for the experiment r1i1p1 as the first part of this work, except for GFDL-CM3, HadGEM2-ES, and IPSL-CM5A-MR for scenario RCP4.5 because these data were unavailable. The experiment identifier indicates which member of an ensemble of parent experiment runs this simulation branched from.

We regridded the extreme temperature indices from all GCMs to a common grid of $2.5^{\circ} \times 2.5^{\circ}$ in southern South America to compare the different models, as Collazo et al. (2021). We applied a first-order conservative remapping procedure (Jones 1999), following Sillmann et al. (2013a). Then, the extreme temperature indices were seasonally averaged: summer (DJF), autumn (MAM), winter (JJA), and spring (SON). In addition, we used the spatially averaged SST in El Niño 3.4 region for each GCM and the ensemble.

2.1 Methodology

2.1.1 Changes in the SST3.4 probability distributions

1 ENSO is one of the main climate drivers, and its changes could affect the global
2 atmospheric circulation. Observed SST3.4 variability has a dominant frequency in the
3 power spectrum of ~3-8 years, associated with ENSO, which is invariant to different
4 record lengths in the historical period (Deser et al. 2006). Therefore, we decided to
5 explore SST3.4 changes in probability density function (PDF) and variability between
6 the 30 years windows in the historical (1976-2005) and near (2031-2060) and far
7 future (2071-2100) by applying the Kolmogorov-Smirnov test (KS-test, Smirnov
8 1939). The null hypothesis of this non-parametric test states that there is no difference
9 between the empirical cumulative distribution functions of two samples, and it is
10 sensitive to differences in both location and shape of the empirical cumulative
11 distribution functions of the two samples. We tested with 5% of a significant level. The
12 discrimination between the near future and the far future seeks to analyze in detail the
13 projected changes under different CO₂ concentrations.

14 In particular, we were interested in determining whether the differences found with
15 KS-test were due to changes in the variances of the SST3.4. For this goal, we used the
16 non-parametric Fligner-Killeen to test if the variances in each of the historical and near
17 and far samples are the same (Fligner & Killeen 1976). This test is robust against
18 departures from normality (Conover et al. 1981).

20 2.1.2 ENSO teleconnections in the future

21 In order to study the link between the ENSO and extreme temperature events in
22 southern South America in the near and far future, we calculated the Spearman
23 correlation (Spearman 1904) and the quantile regression for the 90th percentile

(Koenker 2005) between SST3.4 and extreme temperature indices for the four seasons, as Collazo et al. (2021). The statistical significance of the correlations and regressions was evaluated at a 5% significant level. Before these estimations, the linear trends of the extreme temperature indices and the spatial average of the SST in the central equatorial Pacific were filtered in each future period separately.

Spearman correlation coefficient allows us to measure the non-linear association between two continuous random variables that do not follow a normal distribution. On the other hand, quantile regression explores different aspects of the relationship between a dependent variable and independent variables, for example, the impact of one variable on the tails of the distribution of another by considering the lowest or the highest percentiles. More details can be found in Collazo et al. (2021).

Special attention was paid to the projections made by the GCMs that demonstrated a good performance in representing the ENSO teleconnections in the historical period, according to Taylor diagrams (Taylor 2001), Cohen's kappa coefficient (Cohen 1960), and mapcurves values (Hargrove et al. 2006). The metrics are complementary, so we considered that the GCMs have a good performance if the Taylor diagram showed a correlation above 0.5 and the absolute difference between the modeled and observed standard deviation is less than half the observed standard deviation (and one standard deviation in the case of quantile regression). Furthermore, the GCMs must present a moderate strength of agreement or above (>0.41) according to Cohen's kappa coefficient and a mapcurve value above 0.6 when we compared against observations (Collazo et al. 2021).

We also analyzed the changes in the SLP anomalies pattern between an extended historical period (1936-2005) and the future period (2031-2100) under El Niño and La Niña conditions. We decided to use this extended period in order to obtain more robust SLP composites patterns. The SST3.4 index (after being detrended) was standardized, and a threshold of ± 0.5 was considered to define opposite ENSO phases. Later, we estimated the differences of the SLP anomalies among the two periods. The stippling in the figures indicates that the difference is significant at 1% according to a t-test for the difference of two means.

Finally, with global warming in association with anthropogenic climate change, atmospheric and oceanic variables have begun to include trends related to global warming (Solomon & Newman 2012). Detrending ensures that the timeseries are not biased by the global warming of the historical period and the projected changes (Thompson et al. 2009). Therefore, we repeated the composites of anomaly SLP under El Niño and La Niña but detrended these anomalies in the historical and future periods, separately, since the anthropogenic climate change is even more prominent in the following decades.

3. Results and discussion

3.1 Changes in the SST3.4 probability distributions

Figure 1 shows the PDF of SST in the El Niño 3.4 region according to different GMCs in the historical (1976-2005), near (2031-2060), and far future (2071-2100) periods under the RCP4.5 scenario. The ensemble mean was also considered, as well as the observations in the historical period. These properties were analyzed for the four seasons. Comparison of the historical and far future PDFs of SST3.4 revealed a shift

1 towards warmer conditions under RCP4.5 and a significant difference in all GCMs and
2 seasons according to the K-S test (except GFDL-ESM2M in DJF). On the other hand, the
3 SST3.4 probability distributions of three GCMs in the near future did not differ from
4 the historical period in some seasons (NorESM1-M in SON, CNRM-CM5, and GFDL-
5 ESM2M in DJF). Although the RCP4.5 scenario projects stable SSTs from the mid-
6 century in the Pacific (Hoegh-Guldberg et al. 2014), approximately half of the models
7 show significant changes in PDFs between the near and distant future in the El Niño3.4
8 region.

9 Significant changes in the SST3.4 PDFs could be due to changes in the mean and/or
10 changes in the variations. In particular, we were more interested in changes in the
11 variances since they might produce changes in the correlations with the extreme
12 temperature indices. Under RCP4.5, only a few GCMs revealed significant differences
13 between historical and far future variances (Table S2). Contrary to what we expected,
14 we found more significant differences in the near than in the far future. Regarding the
15 sign of the difference, we saw that it depends on the model.

16 The PDFs of SST3.4 under RCP8.5 are presented in Figure 2. In the far future, the
17 distributions of the SST3.4 are significantly different from the historical ones for all
18 GCMs and seasons. In the near future, only the GFDL-ESM2M model in DJF does not
19 indicate significant differences. Comparison between near and far future PDFs also
20 showed significant differences under this extreme scenario of global warming (except
21 MIROC5 in JJA and SON). Both periods showed a shift towards warmer conditions. On
22 the contrary, most of the GCMs project that the variance of the SST3.4 will not vary in
23 future periods (Table 2). However, agreeing with Cai et al. (2018), we found that

CCSM4 and GDFL-ESM2M models generated reduced SST variability in the eastern Pacific. On the other hand, the ensemble mean simulate an increased variance. Cai et al. (2018) associated this result with the reduced climatological rainfall in the equatorial eastern Pacific projected by CCSM4 and GDFL-ESM2M, in contrast to increased climatological rainfall in the ensemble average. Moreover, they affirm that this increase in variability is largely due to greenhouse-warming-induced intensification of upper-ocean stratification in the equatorial Pacific, which enhances ocean–atmosphere coupling.

3.2 ENSO teleconnections in the future

Projected changes in SST3.4 distributions under future climate will likely continue to alter ENSO teleconnections due to changes in the mid-state of the atmosphere over the globe. Correlations and quantile regression for the 90th percentile between SST3.4 and extreme temperature indices in southern South America were analyzed for scenarios RCP4.5 and RCP8.5 in the near and distant future. Figure 3 shows the most projected category by the GCMs in the near future under RCP4.5. The possible categories are significant positive correlation, significant negative correlation, and no significant correlation. Most GCMs show an agreement that no significant correlations between SST3.4 and extreme temperature indices were expected in the near future, except for significantly positive correlations in northern Chile and its coast and northwestern Argentina for warm nights and days. Moreover, significant negative correlations were observed cold days in northern Chile and for warm days in central Argentina in DJF. At the end of the century, even fewer grid points presented an agreement of significant correlations for RCP4.5 (Figure S1).

1 The agreement of the GCMs in the near future under the RCP8.5 scenario showed
2 similar patterns to those obtained under RCP4.5 (Figure S2). In the far future, the most
3 outstanding difference among scenarios is that the significant negative correlations are
4 widely extended in central Argentina under RCP8.5 in SON (Figure S3). For the other
5 three extremes indices, the majority of GCMs agreed in no significant correlations. In
6 general, all regions that presented agreement between the models show the same sign
7 of correlation and significance as in the historical period (Collazo et al. 2021), except
8 TX90p in SON, where a northward shift of negative correlations is projected.

9 A similar analysis was performed to determine the agreement among the
10 GCMs, considering the slopes of the quantile regression (90th percentile) between
11 SST3.4 and extreme temperature indices. Once more, the models agreed to indicate
12 non-significant slopes for all the extreme indices and stations in the region, with some
13 exceptions in northern Chile (not shown).

14 Both RCPs scenarios indicate that the GCMs project a weaker relationship between the
15 SST3.4 and the extreme indices than the observed in the present climate. Collazo et al.
16 (2021) found significant correlations between SST3.4 and the warm extremes of both
17 minimum and maximum temperatures in a sufficiently extensive region, mainly in
18 winter and spring. For this reason, we are going to focus on analyzing in more detail the
19 projections of these relationships.

20 Considering only the models with the best performance in simulating the relationship
21 in the historical period and the seasons with the strongest ENSO teleconnections
22 (Collazo et al. 2021), we analyzed the future projections. In the historical period, we
23 already highlighted that the warm extremes of the minimum and maximum

1 temperature presented the strongest correlations with SST3.4 in JJA and especially in
2 SON. Austral spring has been suggested as the season when ENSO heating anomalies
3 can trigger changes in the occurrence of midlatitude intraseasonal regimes through
4 Rossby wave propagation, leading to the observed ENSO teleconnection (Cazes-Boezio
5 et al. 2003, Arizmendi & Barreiro 2017). This extratropical teleconnection disappears in
6 summer when the circulation over southeastern South America is dominated by
7 variability in the South Atlantic convergence zone (SACZ). In fall, extratropical South
8 America is again affected by a wave pattern that extends over the South Pacific but is
9 not correlated with ENSO (Cazes-Boezio et al. 2003). Regarding the models with the
10 best performance in the historical period, the results were highly variable according to
11 the season and the extreme index analyzed.

12 The correlations between SST3.4 and TN90p in JJA for the three best models show
13 some differences among them (Figure 4). In the near future under RCP4.5, CSIRO-Mk3-
14 6-0 and GFDL-ESM2M agree that warm conditions in SST3.4 favor an increase of warm
15 nights in northern Chile and northwestern Argentina, while NorESM1-M projected
16 these conditions in central Chile, central-western Argentina, Paraguay, and southern
17 Brazil. In the far future for the RCP4.5 scenario, only GFDL-ESM2M presented a strong
18 significant correlation in the west of the study region. Under RCP8.5, the spatial
19 extension with significant correlations decreases over time, i.e., at the end of the
20 century, the three models show only a few grid points with significant positive
21 correlations. In conclusion, both scenarios and periods indicate that ENSO
22 teleconnections in the future climate seem to weaken and affect a smaller region in
23 southern South America compared to what was observed in the historical period.

1 Regarding the quantile regression of the 90th percentile, we saw that the three models
2 with the best results in the historical period show significant slopes in different regions
3 for each scenario and period (Figure 5). Furthermore, as we observed for correlations,
4 more grid points have significant slopes at the end of the century than what is
5 observed in the near future for the RCP4.5, especially for the GFDL-ESM2M. This
6 behavior is not observed under the RCP8.5 scenario, which shows very few grid points
7 with significant slopes in the far future. We would have expected similar patterns of
8 correlations and slopes in the near future between both scenarios since during this
9 period there are no major differences between the trajectories of greenhouse gas
10 concentrations. However, variable results were found between the scenarios, periods
11 and models that make it difficult to conclude due to the great uncertainty. In
12 particular, for the GFDL model, Yeh & Kirtman (2007) found that it is very little
13 sensitive to the climate change scenario and the noise is the most likely primary source
14 of the decadal modulation of ENSO. On the other hand, the changes between the near
15 and far future projected by CSIRO-Mk3-6-0 under RCP8.5 could be associated with the
16 changes in the variability of SST3.4 (Table 2).

17 The future relationships between SST3.4 and warm nights in SON from the models
18 with the best performance in the historical period are shown in Figure 6. Both
19 scenarios present patterns of correlations very different from those observed in the
20 historical period, even in the near future (Figure 6, upper panel). For this season in the
21 historical period, the observations indicated that warm conditions of SST3.4 favor
22 warm nights in the center and north of Argentina and Chile, Paraguay, south of Brazil,
23 and Uruguay; and a reduction of TN90p in southern Argentina and Chile (Collazo et al.
24 2021). In the near future, the RCP4.5 scenario shows positive correlations only in Chile.

Under the RCP8.5 scenario, the negative correlations extend further north reaching the center of Argentina than those observed in the historical period. On the other hand, the correlations projected under the RCP4.5 scenario for the far future show similar patterns to those observed in the historical period in the north of the study region. Meanwhile, under RCP8.5, the ENSO teleconnection is limited only to some grid points on the continent. The projected slopes of the quantile regression show few grid points with significant values located in different regions according to the scenario and the period (Figure 6, bottom panel). Climate change is also expected to affect the intensity, frequency, and seasonality of the ENSO (Chand & Walsh 2009, Walsh et al. 2012). The reduction of areas with a significant relationship between TN90p and SST3.4 in both seasons (JJA and SON) in the future could also respond to changes in the seasonality of anomalous equatorial Pacific warming. For instance, El Niño events tend to peak toward austral summer (Xie et al. 2010). During this season, the dominant mode of climate variability in South America in the historical period is the SACZ (Cazes-Boezio et al. 2003). Therefore, it remains to analyze whether this intensification of ENSO in the summer will become the dominant mode of variability over South America in the future.

Finally, we analyzed in more detail the correlation between SST3.4 and TX90p in MAM for some selected GMCs since half of the models analyzed presented a good performance in the historical period. Although in the historical period we had only observed significant positive correlations in northern Chile and northwestern Argentina, towards the end of the century, the RCP8.5 scenario simulates significant negative correlations in central Argentina, mainly towards the end of the century

(Figure 7). These correlations imply a change in the pattern of teleconnections in the future.

Coupled climate models exhibit a wide range of behaviors in the simulation of ENSO events and thus varying teleconnection patterns (Meehl et al. 2007a, Langenbrunner&Neelin 2013). In this work, we found changes in the projected correlations patterns between extreme temperature events in southern South America and SST3.4. In the USA, previous studies also found changes in the extreme temperature patterns during future El Niño events probably caused by a shift eastward and northward of El Niño teleconnection patterns in a warmer climate (Meehl et al. 2007b).

Figures 8-9 present the changes in ENSO-teleconnections patterns in the southern hemisphere during warm and cold conditions of the SST3.4 under the RCP4.5, respectively. Similar patterns, although more intense, were found under RCP8.5 (Figures S4 and S5), i.e., El Niño/La Niña related sea level pressure anomalies strengthen with CO₂ as it was observed by Stevenson (2012). Anticyclonic anomalies predominate in the 60-70°S latitude band during the historical period under El Niño events (Figure 8). Consistent with previous studies, we found that the Rossby wave trains excited by tropical convection during El Niño events induce an anticyclonic anomaly over the Amundsen Sea, particularly in JJA and SON (Karoly et al. 1989, Ding et al. 2011, Yiu&Maycock 2020).

The projections show changes in the patterns, e.g., the anticyclonic anomalies are displaced northward, and the Rossby wave train emerging from the equatorial Pacific to the Amundsen Sea is not clearly seen. In particular, in southern Argentina and Chile,

an increase of SLP anomalies is expected in the future during warm conditions of the tropical Pacific. During cold conditions of SST3.4, the SLP presents cyclonic anomalies in the southern Pacific (50-70°S, 200-280°E) in MAM, JJA, and SON in the historical period (Figure 9). This is consistent with the observed patterns for La Niña events. The circulation pattern in the future shows an intensification of the anomalies and a shift in the location of the centers that depend on the analyzed season. In addition, Figures 8-9 suggest a change in the seasonality of ENSO teleconnections in the future. During El Niño events, the anticyclone anomalies in the Amundsen Sea are weaker in winter. On the other hand, during La Niña, teleconnections reach a peak in austral fall and winter, while in the historical period, these maximums occurred in austral winter and spring.

The mean difference of SLP anomalies between El Niño and La Niña in the future tends to be weaker than those of the historical period (Figure 10). Specifically in southern South America, a reduction of the area with significant differences between both phases of the ENSO is observed in all seasons. This weakening of the teleconnection patterns in the future projections may be the reason why, in general, we did not find significant correlations between SST3.4 and the extreme temperatures in southern South America.

By filtering long-term trends, we remove the non-stationarity of the climate system, which is largely associated with anthropogenic climate changes in recent centuries (IPCC 2013). Figure 11 shows ENSO teleconnections after detrended SLP anomalies in the historical and future period under RCP4.5. In this last analysis, unlike what we observe when preserving the trends (Figure 8), the differences between El Niño events in the historical and future periods are not significant. Therefore, the significant

differences found in Figure 8 largely respond to the presence of trends in the time series. However, both figures show a change in the seasonality of ENSO teleconnections in the future, as a weakening of the Rossby wave train is observed in the southern fall and winter during the El Niño events. For La Niña events, there are also no significant differences between the historical period and the future when the SLP anomalies are detrended (Figure S6).

4. Summary and conclusions

We analyzed changes projected by CMIP5 GCMs for the ENSO phenomenon and their link with extreme temperature events in southern South America in a warmer climate. Two scenarios were considered to represent the near (2031-2060) and far (2071-2100) future climate: RCP4.5 and 8.5.

We found that SST3.4 PDFs shift towards warmer conditions. In general, the GCMs agree that the changes between the historical and two future periods are significant for both RCPs. Nevertheless, when we analyzed, in detail, the changes in the variance (since they could affect the correlation values) several models indicate that the variances do not significantly differ from the historical period in neither season.

The GCMs seem to agree on projects for the future that the relationship between SST3.4 and extreme temperatures in southern South America will tend to weaken for all seasons. Only the north of Chile seems to retain some of its teleconnection with ENSO. The combination of internal variability and anthropogenic forcing generates extreme events (Dittus et al. 2018), so the weakening of the ENSO signal in southern South America could imply that anthropogenic forcing is the primary driver of projected

changes in extreme events, although more studies are needed in this regard. Previous studies observed that the smallest changes in temperature indices are simulated in southern South America, particularly in winter, following the small projected changes for the mean temperatures in this region (Meehl et al. 2007a, Sillmann et al. 2013b).

We especially considered those models that presented a better performance in representing SST3.4 and extreme temperature relationships in the historical period. However, these models displayed correlation patterns with little spatial coincidence in future projections. The exception was the projections for the end of the 21st century under the RCP8.5 scenario. In this case, several models simulated significant negative associations between SST3.4 and MAM TX90p in central Argentina.

Finally, changes in surface circulation patterns associated with warm and cold events in the equatorial Pacific were analyzed. We noticed a change in the intensity and the position of midlatitude Rossby waves associated with ENSO convective heating anomalies (Branstator & Selten 2009). Moreover, we observed that the teleconnection patterns of El Niño and La Niña events tend to be more similar in the future. This result could explain the fact that a large part of the observed relationships between extreme temperatures and SST3.4 in the historical period are lost or weaker in the future climate. Moreover, we observed that the temporal changes in ENSO teleconnections are mainly associated with the trends of SLP anomalies under global warming.

This type of study is crucial for a comprehensive understanding of the future changes simulated by GCMs. It remains pending to contrast these results with the new generation of GCMs in the CMIP6. Furthermore, future changes in temperature extremes need to be assessed carefully in relation to other changes in circulation

patterns, such as displacement of subtropical anticyclones (van Oldenborgh et al. 2009, Sillmann&Croc-Maspoli 2009, He et al. 2017, Reboita et al. 2017, Cherchi et al. 2018, Reboita et al. 2019) and other feedback mechanisms like soil moisture (Seneviratne et al. 2006, Jaeger & Seneviratne 2011, Hirschi et al. 2011).

Acknowledgements This research was supported by CONICET PIP 0137-Res 4248/16 from National Council of Scientific and Technical Research, Argentina and UBACyT 2018 20020170100357BA from University of Buenos Aires, Argentina. We acknowledge the Canadian Centre for Climate Modelling and Analysis for providing the climate extreme indices.

References

- Arizmendi F, Barreiro M (2017) ENSO teleconnections in the southern hemisphere: A climate network view. *Chaos* 27(9), 093109. doi:10.1063/1.5004535
- Bellenger H, Guilyardi E, Leloup J, Lengaigne M, Vialard J (2014) ENSO representation in climate models: from CMIP3 to CMIP5. *ClimDyn* 42:1999–2018. <https://doi.org/10.1007/s00382-013-1783-z>
- Branstator G (1984) The relationship between zonal mean flow and quasi-stationary waves in the mid-troposphere. *J Atmos Sci* 41:2163–2178
- Branstator G, Selten F (2009) Modes of variability and climate change. *J Clim* 22: 2639–2658.
- Cai W, Sullivan A, Cowan T (2009) Rainfall teleconnections with Indo-Pacific variability in the WCRP CMIP3 models. *J Clim* 22(19): 5046–5071.
- Cai W, Borlace S, Lengaigne M, van Rensch P, Collins M, Vecchi G, Timmermann A, Santoso A, McPhaden MJ, Lixin W, England MH, Wang G, Guilyardi E, Jin FF (2014). Increasing frequency of extreme El Niño events due to greenhouse warming. *Nature Clim Change* 4: 111–116. <https://doi.org/10.1038/NCLIMATE2100>
- Cai W, Santoso A, Wang G, Yeh S-W, An S-I, Cobb KM, Collins M, Guilyardi E, Jin F-F, Kug J-S, Lengaigne M, McPhaden MJ, Taka-hashi K, Timmermann A, Vecchi G, Watanabe M, Wu L (2015) ENSO and greenhouse warming. *Nature Clim Change* 5:849–859. <https://doi.org/10.1038/nclimate2743>

- 1 Cai W, Wang G, Dewitte B, Wu L, Santoso A, Takahashi K, Yang Y, CarréricA, McPhaden MJ
2 (2018) Increased variability of eastern Pacific El Niño under greenhouse warming.
3 Nature564(7735): 201–206. doi:10.1038/s41586-018-0776-9
4
- 5 Capotondi A, Wittenberg AT, Newman M, Di Lorenzo E, Yu J-Y, Braconnot
6 P, Cole J, Dewitte B, Giese B, Guilyardi E, Jin F-F, Karnauskas K,
7 Kirtman B, Lee T, Schneider N, Xue Y, Yeh S-W (2015) Understanding
8 ENSO diversity. Bull Am Meteor Soc 96:921–938.
9 <https://doi.org/10.1175/BAMS-D-13-00117> .1
10
- 11 Carréric A, Dewitte B, Cai W, CapotondiA, Takahasi K, Yeh S-W, Wang G, Guémas V(2020) Change in
12 strong Eastern Pacific El Niño events dynamics in the warming climate. ClimDyn 54: 901–918.
13 <https://doi.org/10.1007/s00382-019-05036-0>
14
- 15 Cazes-Boezio G, Robertson AW, Mechoso CR (2003) Seasonal dependence of ENSO teleconnections over
16 South America and relationships with precipitation in Uruguay. J Clim 16(8): 1159–1176
17
- 18 Chand SS,Walsh KJE (2011) Influence of ENSO on tropical cyclone intensity in the Fiji region. J
19 Clim 24: 4096–4108.<https://doi.org/10.1175/2011JCLI4178.1>
20
- 21 Cherchi A, Ambrizzi T, Behera S, Vasques Freitas AC, Morioka Y, Zhou T (2018) The Response of
22 Subtropical Highs to Climate Change. CurrClim Change Rep 4, 371–
23 382.<https://doi.org/10.1007/s40641-018-0114-1>
24
- 25 Christensen JH, Krishna Kumar K, AldrianE, An S-I, Cavalcanti IFA,de Castro M, Dong W, Goswami P, Hall
26 A, Kanyanga JK, Kitoh A, Kossin J, LauN-C, Renwick J, Stephenson DB, XieS-P,ZhouT (2013) Climate
27 Phenomena and their Relevance for Future Regional Climate Change. In: Climate Change 2013:
28 The Physical Science Basis. Contribution of Working Group I to the Fifth Assessment Report of the
29 Intergovernmental Panel on Climate Change [Stocker, T.F., D. Qin, G.-K. Plattner, M. Tignor, S.K.
30 Allen, J. Boschung, A. Nauels, Y. Xia, V. Bex and P.M. Midgley (eds.)]. Cambridge University Press,
31 Cambridge, United Kingdom and New York, NY, US
32
- 33 Cohen J (1960) A Coefficient of Agreement for Nominal Scales. Educational and Psychological
34 Measurement 20 (1): 37-46. DOI: 10.1177/001316446002000104
35
- 36 Collazo S,Barrucand M,Rusticucci M (2021). Association between El Niño and extreme temperatures in
37 southern South America in CMIP5 models. Part 1: model evaluation in the present climate. Clim
38 Res 83: 111-132. DOI: <https://doi.org/10.3354/cr01639>.
39
- 40 Collins M, An SI, Cai W, Ganachaud A, Guilyardi E, Jin FF,Jochum M, Lengaigne M, Power S, Timmermann
41 A, Vecchi G, Wittenberg A (2010) The impact of global warming on the tropical Pacific Ocean and
42 El Niño. Nat Geosci 3(6): 391–397. <https://doi.org/10.1038/ngeo868>
43
44
- 45 Conover WJ, Johnson ME, Johnson MM (1981) A comparative study of tests for homogeneity of
46 variances, with applications to the outer continental shelf bidding data. Technometrics 23: 351--
47 361. 10.2307/1268225.
48
- 49 Deser C, Capotondi A, Saravanan R, Phillips AS (2006) Tropical Pacific and Atlantic Climate Variability in
50 CCSM3. J Clim19(11): 2451–2481. doi:10.1175/jcli3759.1
51
- 52 Ding Q, Steig EJ, Battisti DS, Küttel M (2011). Winter warming in West Antarctica caused by central
53 tropical Pacific warming. Nat Geosci 4(6),398. DOI: 10.1038/ngeo1129
54
- 55 Dittus AJ, Karoly DJ, Donat MG, Lewis SC,Alexander LV (2018) Understanding the role of sea surface
56 temperature-forcing for variability in global temperature and precipitation extremes. Weather
57 ClimExtrem 21: 1-9. DOI: 10.1016/j.wace.2018.06.002
58

- 1 Fligner MA, Killeen TJ (1976) Distribution-Free Two-Sample Tests for Scale. *J Amer Statist Assoc* 71: 210-
2 213
3
4
- 5 Guilyardi E, Cai W, Collins M, Fedorov A, Jin F-F, Kumar A, Sun D-Z, Wittenberg A (2012) New strategies
6 for evaluating ENSO processes in climate models. *Bull Am Meteorol Soc* 93:235–238
7
- 8 Halpert MS, Ropelewski CF (1992) Surface temperature patterns associated with the Southern
9 Oscillation. *J Clim* 5: 577–593, doi:10.1175/1520-0442(1992)005<0577:STPAWT>2.0.CO;2.
10
- 11 Hargrove WW, Hoffman FM, Hessburg PF (2006) Mapcurves: a quantitative method for comparing
12 categorical maps. *J Geogr Syst* 8, 187. <https://doi.org/10.1007/s10109-006-0025-x>
13
- 14 He C, Wu B, Zou L, Zhou T (2017) Responses of the summertime subtropical anticyclones to global
15 warming. *J Clim* 30: 6465–6479. doi: 10.1175/JCLI-D-16-0529.1
16
- 17 Hirschi M, Seneviratne SI, Alexandrov V, Boberg F, Boroneant C, Christensen OB, Formayer H, Orłowsky B,
18 Stepanek P (2011) Observational evidence for soil-moisture impact on hot extremes in
19 southeastern Europe. *Nature Geosci* 4(1): 17–21
20
- 21 Hoegh-Guldberg O, Cai R, Poloczanska ES, Brewer PG, Sundby S, Hilmi K, Fabry VJ, Jung S (2014) The
22 Ocean. In: *Climate Change 2014: Impacts, Adaptation, and Vulnerability. Part B: Regional Aspects.*
23 *Contribution of Working Group II to the Fifth Assessment Report of the Intergovernmental Panel*
24 *on Climate Change* [Barros VR, Field CB, Dokken DJ, Mastrandrea MD, Mach KJ, Bilir TE,
25 Chatterjee M, Ebi KL, Estrada YO, Genova RC, Girma B, Kissel ES, Levy AN, MacCracken S,
26 Mastrandrea PR, White LL (eds.)]. Cambridge University Press, Cambridge, United Kingdom and
27 New York, NY, USA, pp. 1655–1731.
28
- 29 IPCC (2013) *Climate Change 2013: The Physical Science Basis. Contribution of Working Group I to the*
30 *Fifth Assessment Report of the Intergovernmental Panel on Climate Change* [Stocker TF, Qin D,
31 Plattner G-K, Tignor M, Allen SK, Boschung J, Nauels A, Xia Y, Bex V, Midgley PM (eds.)].
32 Cambridge University Press, Cambridge, United Kingdom and New York, NY, USA, 1535 pp.
33
- 34 IPCC (2014) *Climate Change 2014: Synthesis Report. Contribution of Working Groups I, II and III to the*
35 *Fifth Assessment Report of the Intergovernmental Panel on Climate Change* [Core Writing Team,
36 Pachauri RK and Meyer LA (eds.)]. IPCC, Geneva, Switzerland, 151 pp.
37
- 38 Jaeger EB, Seneviratne SI (2011) Impact of soil moisture–atmosphere coupling on European climate
39 extremes and trends in a regional climate model. *Clim Dyn* 36: 1919–1939.
40 <https://doi.org/10.1007/s00382-010-0780-8>
41
- 42 Jones PW (1999) First- and Second-Order Conservative Remapping Schemes for Grids in Spherical
43 Coordinates. *Mon Weather Rev* 127 (9): 2204–2210.
44
- 45 Karoly DJ (1989) Southern Hemisphere Circulation Features Associated with El Niño–Southern Oscillation
46 Events. *J Clim* 2: 1239–1252, doi:10.1175/1520-0442(1989)002<1239:shcfaw>2.0.co;2
47
- 48 Kim ST, Yu JY (2012) The two types of ENSO in CMIP5 models. *Geophys Res Lett* 39, L11704,
49 doi:10.1029/2012GL052006.
50
- 51 King AD, van Oldenborgh GJ, Karoly DJ (2016) Climate change and El Niño increase likelihood of
52 Indonesian heat and drought. *Bull Am Meteorol Soc* 97: S113–
53 S117. <https://doi.org/10.1175/BAMS-D-16-0164.1>
54
- 55 Kodra E, Ganguly A (2014) Asymmetry of projected increases in extreme temperature distributions. *Sci*
56 *Rep* 4, 5884. <https://doi.org/10.1038/srep05884>
57
- 58 Koenker R (2005). *Quantile Regression. Econometric Society Monographs.* Cambridge University Press.

- 1
- 2 Langenbrunner B,NeelinJD (2013). Analyzing ENSO teleconnections in CMIP models as a measure of
- 3 model fidelity in simulating precipitation. J Clim 26: 4431–4446.
- 4
- 5 López-Franca N, Zaninelli PG,Carril AF, Menendez CG, Sánchez E (2016) Changes in temperature
- 6 extremes for 21st century scenarios over South America derived from a multi-model ensemble of
- 7 regional climate models.Clim Res 68; 2-3: 151-167. DOI: <https://dx.doi.org/10.3354/cr01393>
- 8
- 9 Meehl GA, Branstator GW, Washington WM (1993) Tropical Pacific interannual variability and CO2
- 10 climate change. J Clim 6:42–63
- 11
- 12 Meehl GA, Teng H, Branstator G (2006) Future changes of El Niño in two global coupled climate models.
- 13 ClimDyn 26:549–566
- 14
- 15 Meehl GA, Stocker TF, Collins WD, Friedlingstein P, Gaye AT, Gregory JM, ... Zhao Z-C. (2007a) Global
- 16 Climate Projections. In S. Solomon, et al. (Eds.), Climate change 2007: The physical science basis.
- 17 Contribution ofworking group I to the 4th assessment report ofthe intergovernmental panel on
- 18 climate change (747–845). Cambridge, United Kingdom and New York: Cambridge University
- 19 Press.
- 20
- 21 Meehl GA, Tebaldi C, Teng H, Peterson TC (2007b) Current and future US weather extremes and El Niño.
- 22 Geophys Res Lett34, L20704. <https://doi.org/10.1029/2007GL031027>
- 23
- 24 Perry SJ, McGregor S, Gupta AS, England MH (2017) Future changes to El Niño–Southern Oscillation
- 25 temperature and precipitation teleconnections. Geophys Res Lett, 44, 10,608–10,616.
- 26 <https://doi.org/10.1002/2017GL074509>
- 27
- 28 Power S, Delage F, Chung C, Kociuba G, Keay K (2013) Robust twenty-first-century projections of El Niño
- 29 and related precipitation variability. Nature 502: 541–545. <https://doi.org/10.1038/nature12580>
- 30
- 31 Rayner NA, Parker DE, Horton EB, Folland CK, Alexander LV, Rowell DP, Kent EC, Kaplan A (2003) Global
- 32 analyses of sea surface temperature, sea ice, and night marine air temperature since the late
- 33 nineteenth century. J Geophys Res Vol. 108, No. D14, 4407 10.1029/2002JD002670
- 34
- 35 Reboita MS, Ambrizzi T, Silva BA, Pinheiro RF, da Rocha RP (2019) The South Atlantic Subtropical
- 36 Anticyclone: Present and Future Climate. Front. Earth Sci. 7:8. DOI=10.3389/feart.2019.00008
- 37
- 38 Reboita MS, Amaro TR, de Souza MR (2017). Winds: intensity and power density simulated by RegCM4
- 39 over South America in present and future climate. ClimDyn 51: 187–205. doi: 10.1007/s00382-
- 40 017-3913-5
- 41
- 42 Ropelewski CF, Halpert M (1987) Global and regional scale precipitation
- 43 patterns associated with the El Niño/Southern Oscillation. Mon
- 44 Weather Rev 115: 1606–1626. [https://doi.org/10.1175/1520-](https://doi.org/10.1175/1520-0493(1987)115%3c1606:GARSP%3e2.0.CO;2)
- 45 [0493\(1987\)115%3c1606:GARSP P%3e2.0.CO;2](https://doi.org/10.1175/1520-0493(1987)115%3c1606:GARSP%3e2.0.CO;2)
- 46
- 47 Seneviratne SI, Lüthi D, Litschi M, Schär C (2006) Land–atmosphere coupling and climate change in
- 48 Europe. Nature 443:205–209
- 49
- 50 Seneviratne SI, Nicholls N, Easterling D, Goodess CM, Kanae S, Kossin J, Luo Y, Marengo J, McInnes K,
- 51 Rahimi M,Reichstein M, Sorteberg A, Vera C,Zhang X(2012) Changes in climate extremes and
- 52 their impacts on the naturalphysical environment. In: Managing the Risks of Extreme Events and
- 53 Disasters to Advance Climate Change Adaptation[Field CB, Barros V, Stocker TF, Qin D, Dokken
- 54 DJ, Ebi KL, Mastrandrea MD, Mach KJ, Plattner G-K, Allen SK,Tignor M, Midgley PM (eds.)]. A
- 55 Special Report of Working Groups I and II of the Intergovernmental Panel on ClimateChange
- 56 (IPCC). Cambridge University Press, Cambridge, UK, and New York, NY, USA, pp. 109-230.
- 57

- Sillmann J, Croci-Maspoli M (2009). Present and future atmospheric blocking and its impact on European mean and extreme climate. *Geophys Res Lett* 36, L10702, doi:10.1029/2009GL038259.
- Sillmann J, Kharin VV, Zhang X, Zwiers FW, Bronaugh D (2013a) Climate extremes indices in the CMIP5 multimodel ensemble: Part 1. Model evaluation in the present climate. *J Geophys Res Atmos* 118 (4): 1716-1733. DOI: 10.1002/jgrd.50203
- Sillmann J, Kharin VV, Zwiers FW, Zhang X, Bronaugh D (2013b). Climate extremes indices in the CMIP5 multimodel ensemble: Part 2. Future climate projections. *J Geophys Res Atmos* 118 (6): 2473-2493. DOI:10.1002/jgrd.50188
- Smirnov NV (1939) Estimate of deviation between empirical distribution functions in two independent samples. (Russian). *Bull Moscow Univ* 2 (2): 3–16 (6.1, 6.2).
- Solomon A, Newman M (2012). Reconciling disparate twentieth-century Indo-Pacific Ocean temperature trends in the instrumental record. *Nature Climate Change* 2: 691-699.
- Spearman C (1904) The Proof and Measurement of Association between Two Things. *Am J Psychol* 15 (1): 72-101. URL: <http://www.jstor.org/stable/1412159>
- Sterl A, van Oldenborgh GJ, Hazeleger W, Burgers G (2007) On the robustness of ENSO teleconnections. *ClimDyn* 28:181–197. doi: 10.1007/s00382-007-0251-z
- Stevenson SL (2012) Significant changes to ENSO strength and impacts in the twenty-first century: Results from CMIP5. *Geophys Res Lett* 39, L17703. <https://doi.org/10.1029/2012GL052759>
- Stevenson S, Fox-Kemper B, Jochum M, Neale R, Deser C, Meehl G (2012) Will there be a significant change to El Niño in the twenty-first century? *J. Climate* 25: 2129–2145, <https://doi.org/10.1175/JCLI-D-11-00252.1>.
- Taschetto AS, Ummenhofer CC, Stuecker MF, Dommenges D, Ashok K, Rodrigues RR and Yeh S-W (2020). ENSO Atmospheric Teleconnections. In *El Niño Southern Oscillation in a Changing Climate* (eds M.J. McPhaden, A. Santoso and W. Cai). <https://doi.org/10.1002/9781119548164.ch14>
- Taylor KE (2001) Summarizing multiple aspects of model performance in a single diagram. *J Geophys Res* 106: 7183–7192
- Taylor KE, Stouffer R J, Meehl GA (2012). An overview of CMIP5 and the experiment design. *Bull Am Meteorol Soc* 93(4), 485–498. <https://doi.org/10.1175/BAMS-D-11-00094.1>
- Thompson DWJ, Wallace JM, Jones PD, Kennedy JJ (2009). Identifying Signatures of Natural Climate Variability in Time Series of Global-Mean Surface Temperature: Methodology and Insights. *J Clim* 22(22): 6120-6141. Retrieved Jun 14, 2021, from <https://journals.ametsoc.org/view/journals/clim/22/22/2009jcli3089.1.xml>
- Trenberth KE et al (1998) Progress during TOGA in understanding and modelling global teleconnections associated with tropical sea surface temperature. *J Geophys Res* 103:14291–14324
- van Oldenborgh GJ, Drijfhout S, van Ulden A, Haarsma R, Sterl A, Severijns C, Hazeleger W, Dijkstra H (2009) Western Europe is warming much faster than expected. *Climate of the Past*, 5(1), 1-12
- van Vuuren DP, Edmonds J, Kainuma M. et al. (2011) The representative concentration pathways: an overview. *Clim Change* 109, 5. <https://doi.org/10.1007/s10584-011-0148-z>

- 1 Walsh KJE, McInnes KL, McBride JL (2012). Climate change impacts on tropical cyclones and extreme sea
2 levels in the South Pacific — A regional assessment. *GlobPlanetChange* 80-81: 149–
3 164. doi:10.1016/j.gloplacha.2011.10.006
4
5
6 Wang B, Luo X, Yang Y-M, Sun W, Cane M A, Cai W, Yeh S-W, Liu, J. (2019). Historical change of El Niño
7 properties sheds light on future changes of extreme El Niño. *Proceedings of the National*
8 *Academy of Sciences*, 201911130. doi:10.1073/pnas.1911130116
9
10 Xie S, Deser C, Vecchi GA, Ma J, Teng H, Wittenberg AT (2010) Global Warming Pattern Formation: Sea
11 Surface Temperature and Rainfall. *J Clim* 23(4): 966-986.
12 <https://doi.org/10.1175/2009JCLI3329.1>
13
14 Yeh SW, Kirtman B (2007) ENSO amplitude changes due to climate change projections in different
15 coupled models. *J Clim* 20: 203–217. <https://doi.org/10.1175/JCLI4001.1>
16
17 Yeh SW, Cai W, Min SK, McPhaden MJ, Dommenges D, Dewitte B, Collins M, Ashok K, An SI, Yim BY, Kug
18 JS (2018) ENSO atmospheric teleconnections and their response to greenhouse gas forcing. *Rev*
19 *Geophys* 56:185–206. <https://doi.org/10.1002/2017RG000568>
20
21 Yiu YYS, Maycock AC. (2020). The linearity of the El Niño teleconnection to the Amundsen Sea region. *Q*
22 *J R Meteorol Soc*. doi:10.1002/qj.3731
23
24
25

Tables:

Label	Index name	Description
TN10p	Cold nights	Percentage of days in a month when daily minimum temperature is below the 10 th percentile centered on a 5 day window
TN90p	Warm nights	Percentage of days in a month when daily minimum temperature is above the 90 th percentile centered on a 5 day window
TX10p	Cold days	Percentage of days in a month when daily maximum temperature is below the 10 th percentile centered on a 5 day window
TX90p	Warm days	Percentage of days in a month when daily maximum temperature is above the 90 th percentile centered on a 5 day window

Table 1: Four Extreme Temperature Indices Recommended by the ETCCDI.

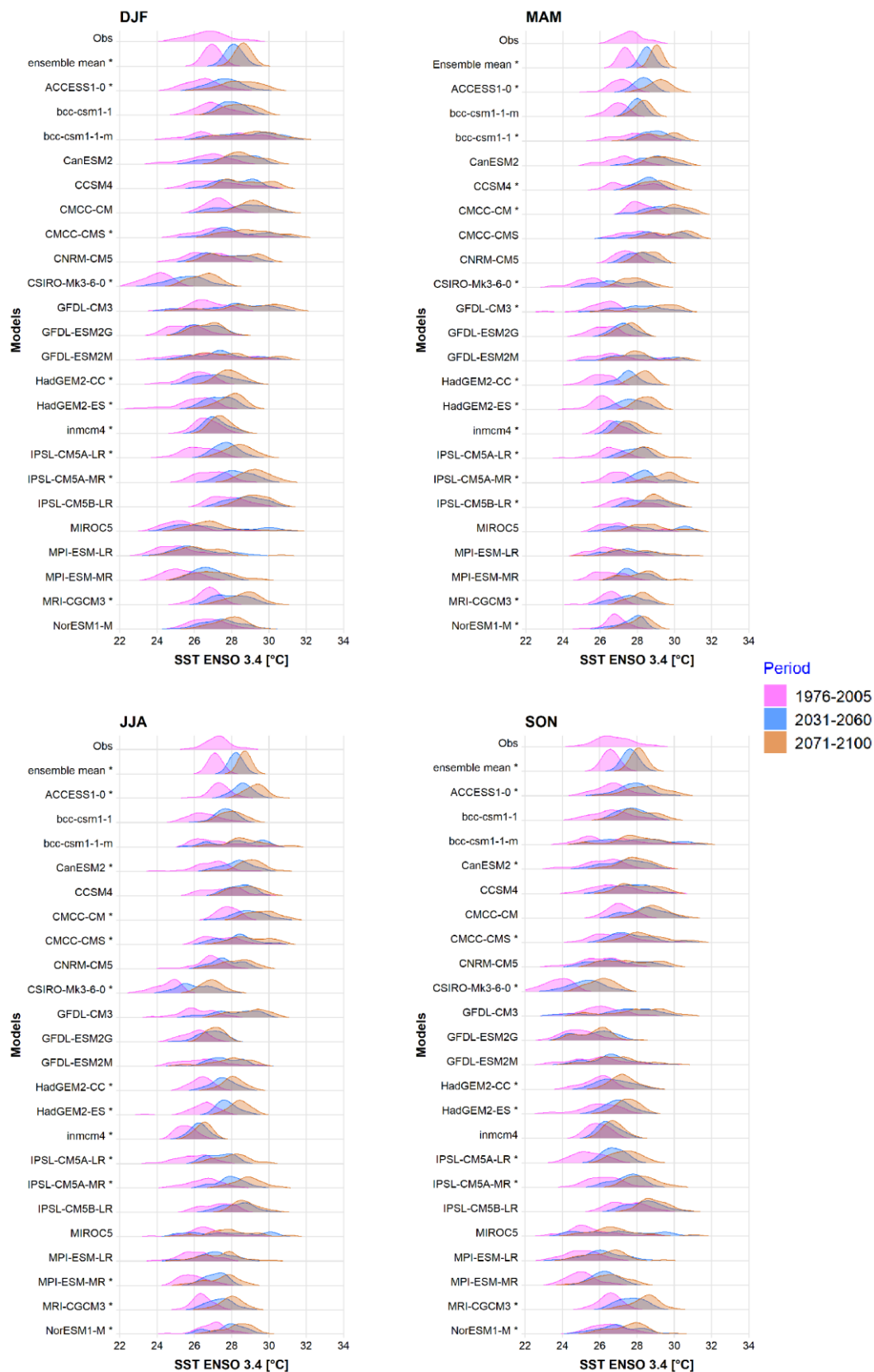
	RCP8.5				RCP8.5			
	Nearfuture (2031-2060)				Far future (2071-2100)			
	MAM	JJA	SON	DJF	MAM	JJA	SON	DJF
ACCESS1-0	0.12	0.01	-0.08	0.14	0.16	0.13	0.06	0.14
bcc-csm1-1	0.05	-0.30	-0.36	-0.14	0.01	-0.24	-0.14	-0.11
CanESM2	-0.09	-0.22	-0.14	0.16	0.11	0.06	-0.03	-0.33
CCSM4	-0.77	-0.72	-1.00	-1.06	-0.69	-0.55	-0.53	-0.68
CMCC-CM	0.33	0.43	0.68	0.61	0.62	0.59	0.59	0.77
CMCC-CMS	0.24	0.44	0.42	0.63	0.25	-0.03	0.06	-0.19
CNRM-CM5	0.02	0.12	0.84	0.35	0.13	0.12	0.47	0.17
CSIRO-Mk3-6-0	0.08	0.43	0.16	-0.06	0.79	0.62	0.41	0.64
GFDL-CM3	0.46	-0.01	0.76	1.16	0.32	-0.15	0.26	0.56
GFDL-ESM2G	-0.14	0.30	0.39	-0.19	-0.03	0.00	-0.31	-0.53
GFDL-ESM2M	-0.06	-0.06	-0.70	-0.55	-1.19	-0.53	-1.72	-2.17
HadGEM2-CC	-0.05	0.18	0.11	-0.19	0.03	0.29	0.20	0.06
HadGEM2-ES	0.41	-0.13	-0.44	-0.41	0.11	-0.18	-0.33	-0.56
inmcm4	-0.01	0.04	0.09	0.03	-0.08	-0.03	-0.01	-0.02
IPSL-CM5A-LR	-0.20	-0.26	0.04	0.01	0.00	0.01	0.00	-0.16
IPSL-CM5A-MR	0.12	-0.19	-0.29	-0.12	0.05	-0.28	-0.36	-0.30

IPSL-CM5B-LR	0.25	0.26	0.05	0.14	0.56	0.29	0.49	0.36
MIROC5	0.52	0.85	1.00	1.57	-0.35	0.56	0.96	0.92
MPI-ESM-LR	0.70	0.38	0.64	1.07	0.48	0.43	0.77	0.95
MPI-ESM-MR	0.30	0.56	0.62	0.44	0.76	0.44	0.54	1.19
MRI-CGCM3	0.33	0.29	0.56	0.54	0.49	0.39	0.62	0.81
NorESM1-M	-0.13	-0.22	-0.02	-0.22	-0.09	-0.28	0.10	-0.28
ensemble mean	0.08	0.06	0.06	0.06	0.09	0.07	0.03	0.05

Table 2: Idem Table 3 for RCP8.5 scenario.

ACCEPTED VERSION

1 Figures:



- 1 Figure 1: Probability distributions of the sea surface temperatures in El Niño3.4 region in the
- 2 historical, near and far future periods under RCP4.5 scenario. Significant differences between
- 3 near and far future distributions are indicated with an asterisk.

ACCEPTED VERSION

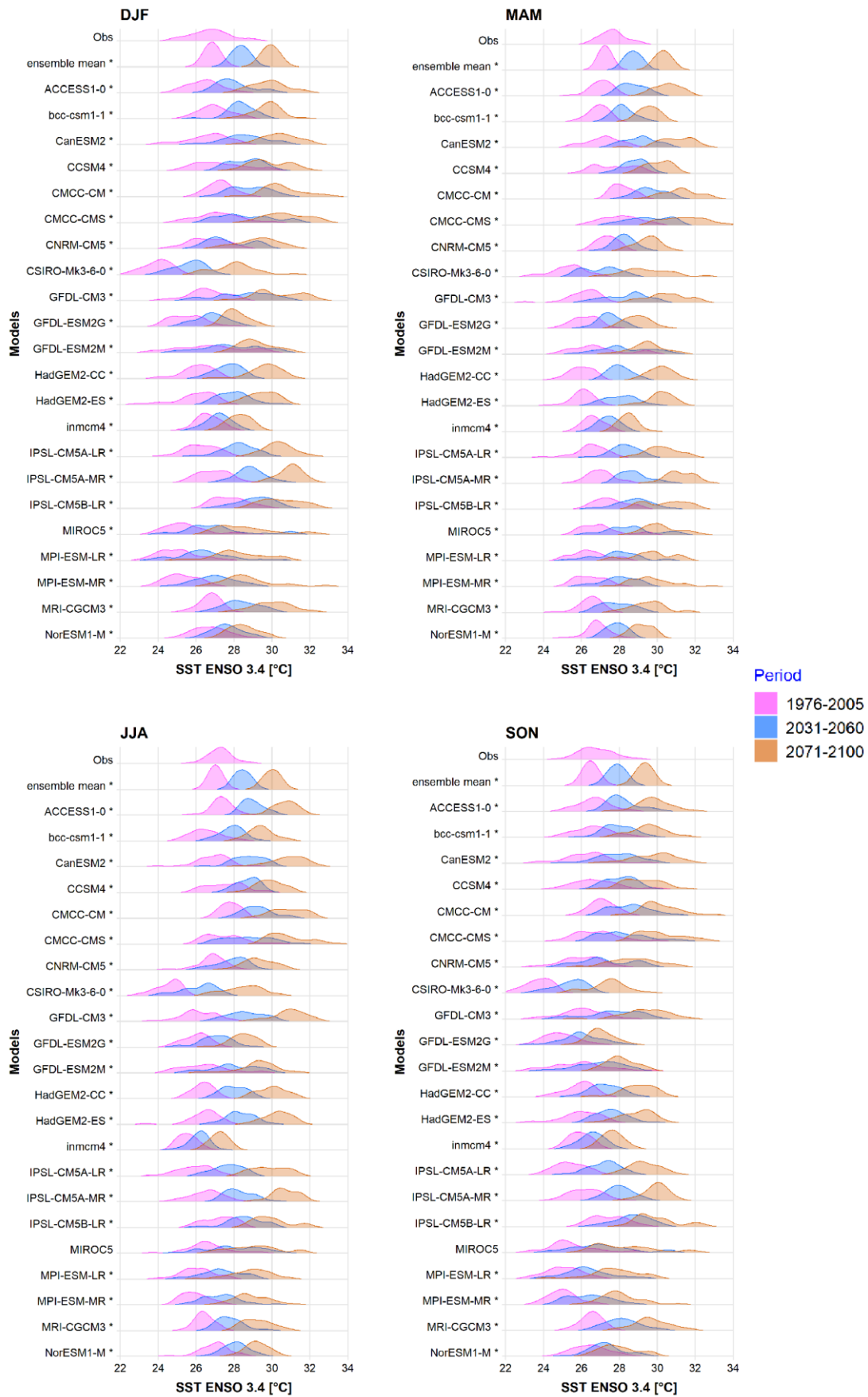
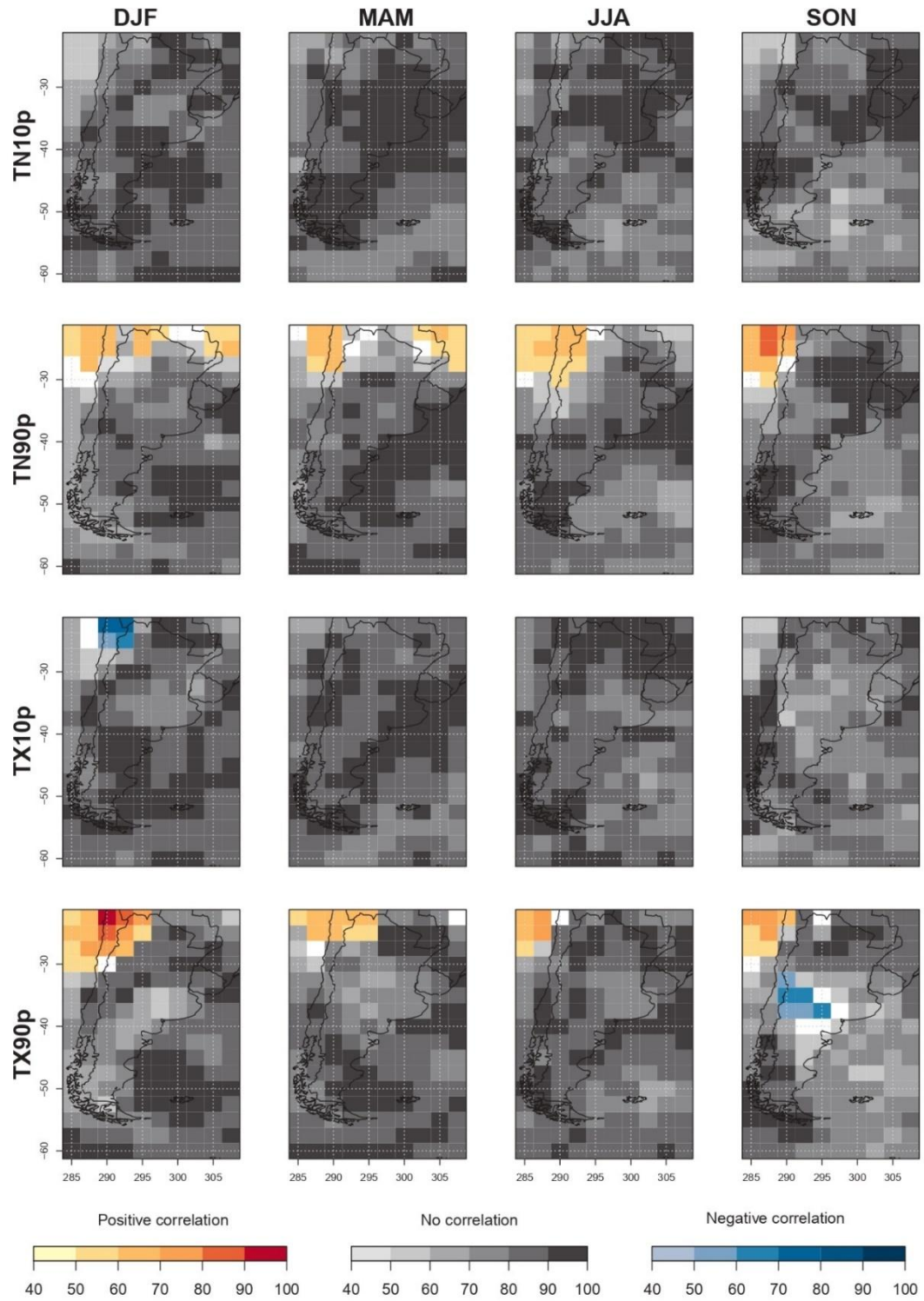


Figure 2: Idem Figure 1 under RCP8.5 scenario.

1



2

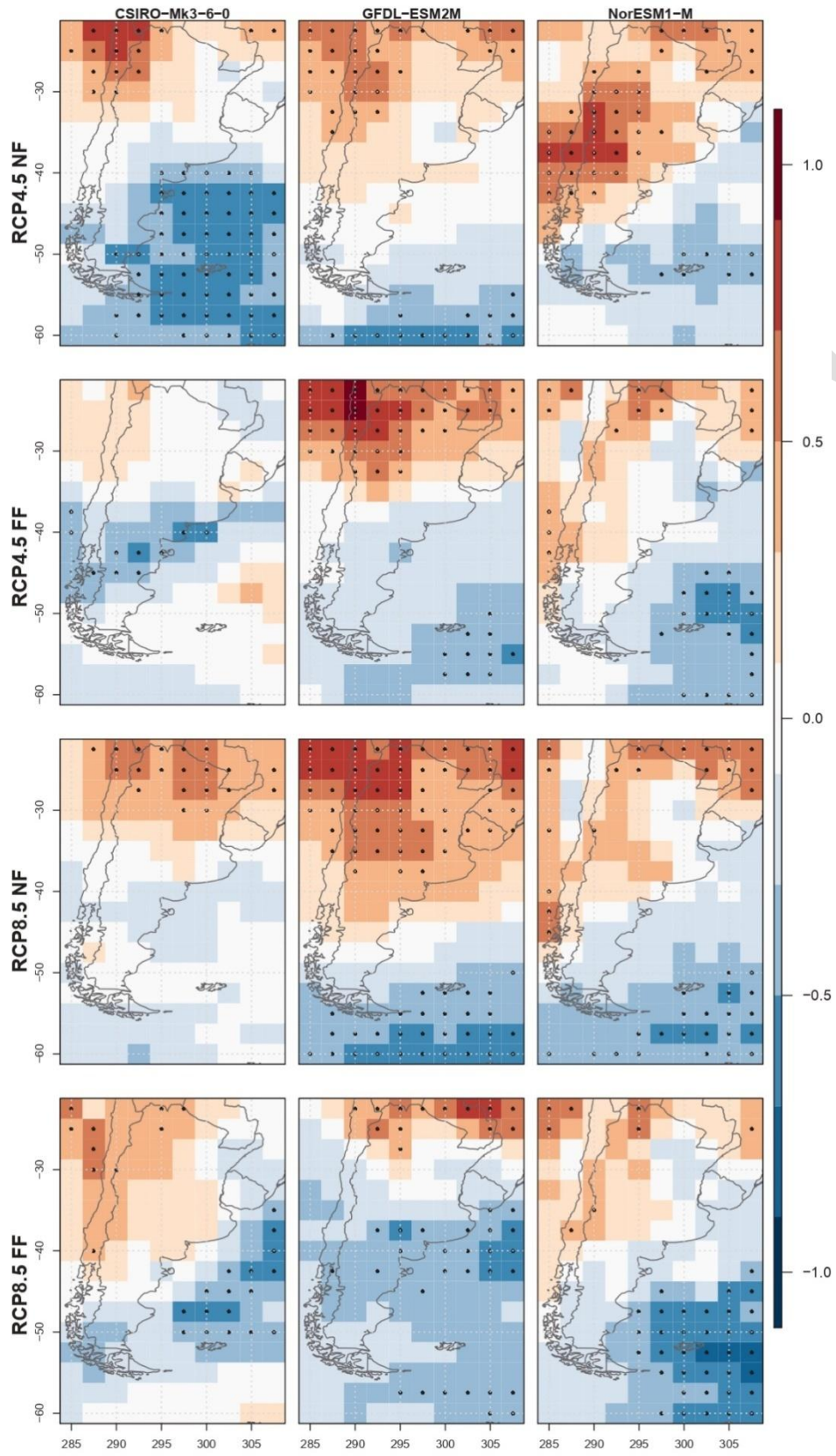
3

4

5

6

Figure 3: Agreement between GCMs in the projected correlations for RCP4.5 in the near future. Percentage of the most projected category, being the three categories positive significant correlation, negative significant correlation, and no significant correlation at 95% confidence level.



1 Figure 4: Correlation between modeled SST in El Niño 3.4 region and warm nights index in JJA for the
 2 near (NF) and far future (FF) under the RCP4.5 and RCP8.5 scenarios and for the GCMs with best
 3 performance (dotted regions indicate significant correlation at the 0.05 significance level).

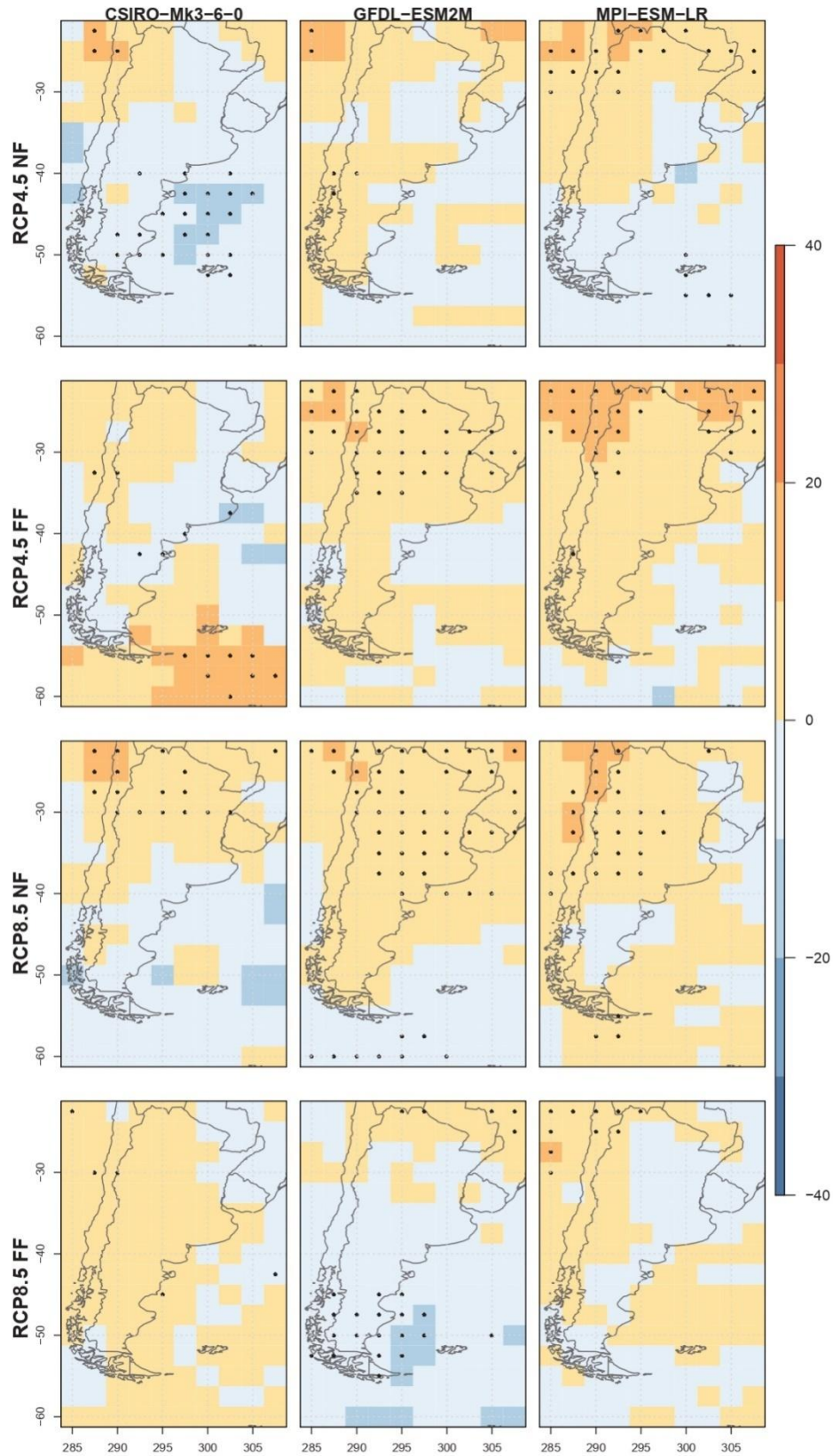
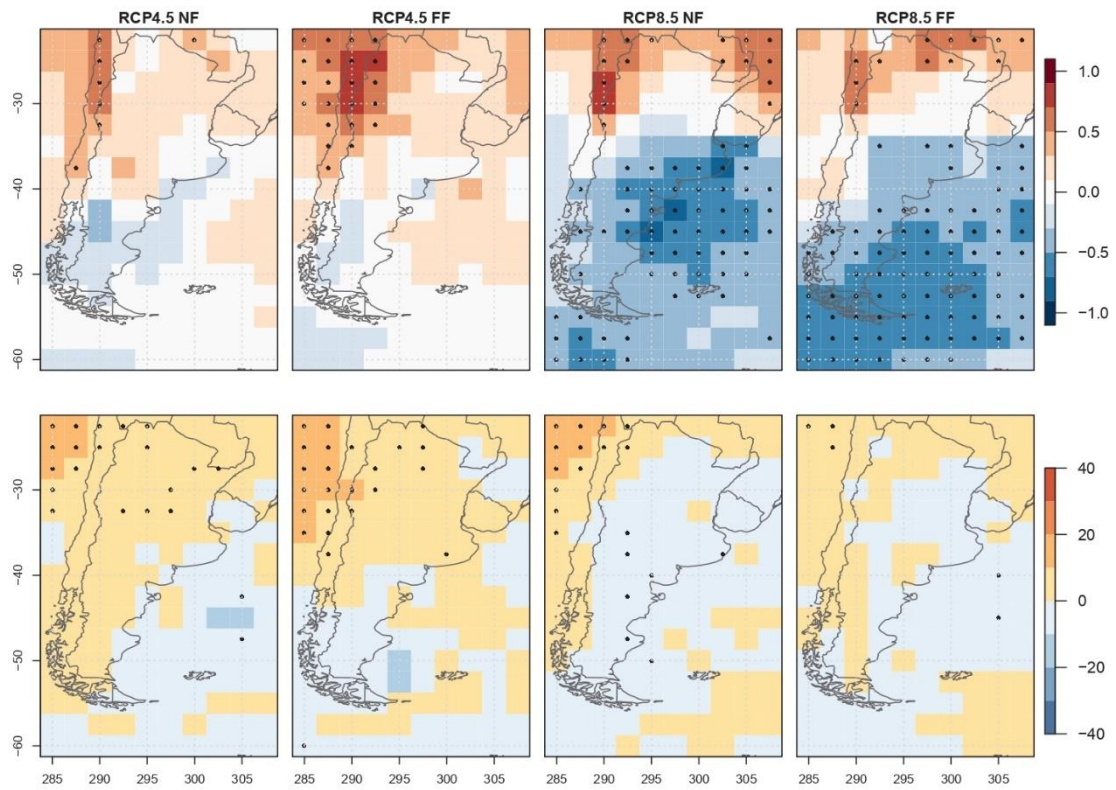


Figure 5: Slope of the 90th percentile regression between modeled SST in El Niño 3.4 region and warm nights index [%°C⁻¹] in JJA for the near (NF) and far future (FF) under the RCP4.5 and RCP8.5 scenarios and for the GCMs with best performance (dotted regions indicate significant correlation at the 0.05 significance level).

6



7

Figure 6: Correlation between modeled SST in El Niño 3.4 region and warm nights index in SON for the near (NF) and far future (FF) under the RCP4.5 and RCP8.5 scenarios and for the CNRM-CM5 (dotted regions indicate significant correlation at the 0.05 significance level. upper row). Slope of the 90th percentile between modeled SST in El Niño 3.4 region and warm nights index [%°C⁻¹] in SON for the near (NF) and far future (FF) under the RCP4.5 and RCP8.5 scenarios and for the MPI-ESM-LR (dotted regions indicate significant correlation at the 0.05 significance level. lower row).

14

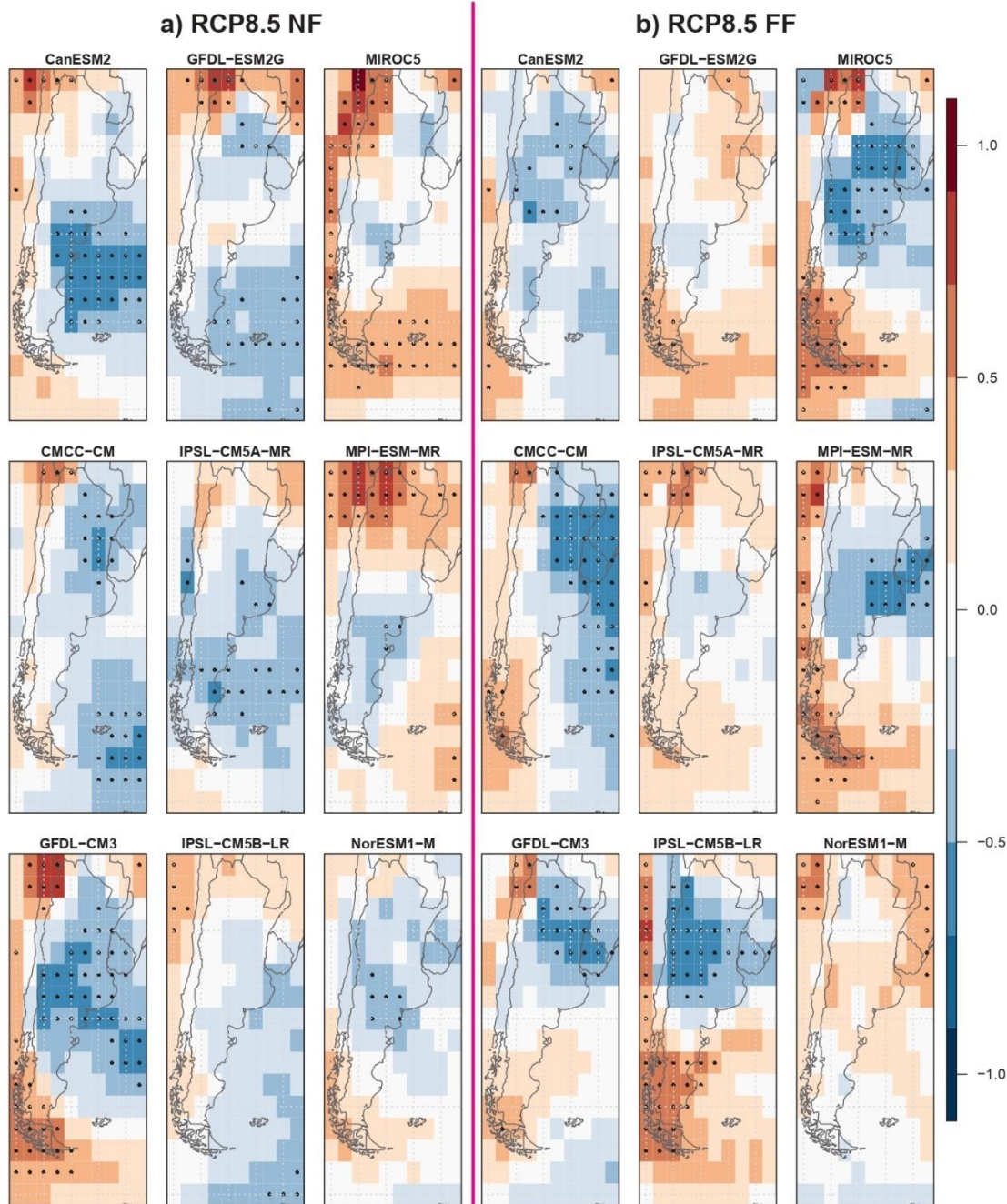


Figure 7: Correlation between modeled SST in El Niño 3.4 region and warm days index in MAM for the near (NF. a) and far future (FF. b) under RCP8.5 scenario and for the GCMs with best performance (dotted regions indicate significant correlation at the 0.05 significance level).

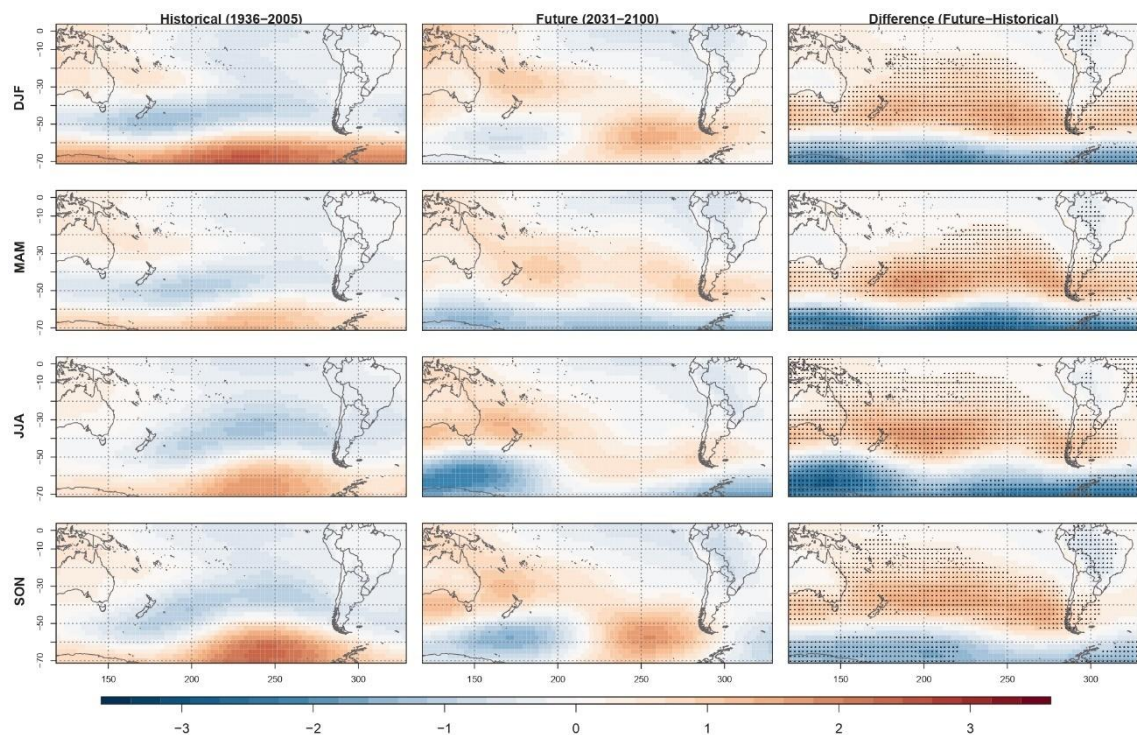


Figure 8: Composites of the sea level pressure anomalies [hPa] during warm conditions of the standardized SST3.4 in the historical (1936-2005) and future (2031-2100) periods under RCP4.5 scenario. The differences among those periods are also show. Stippling indicates significant difference at 1%.

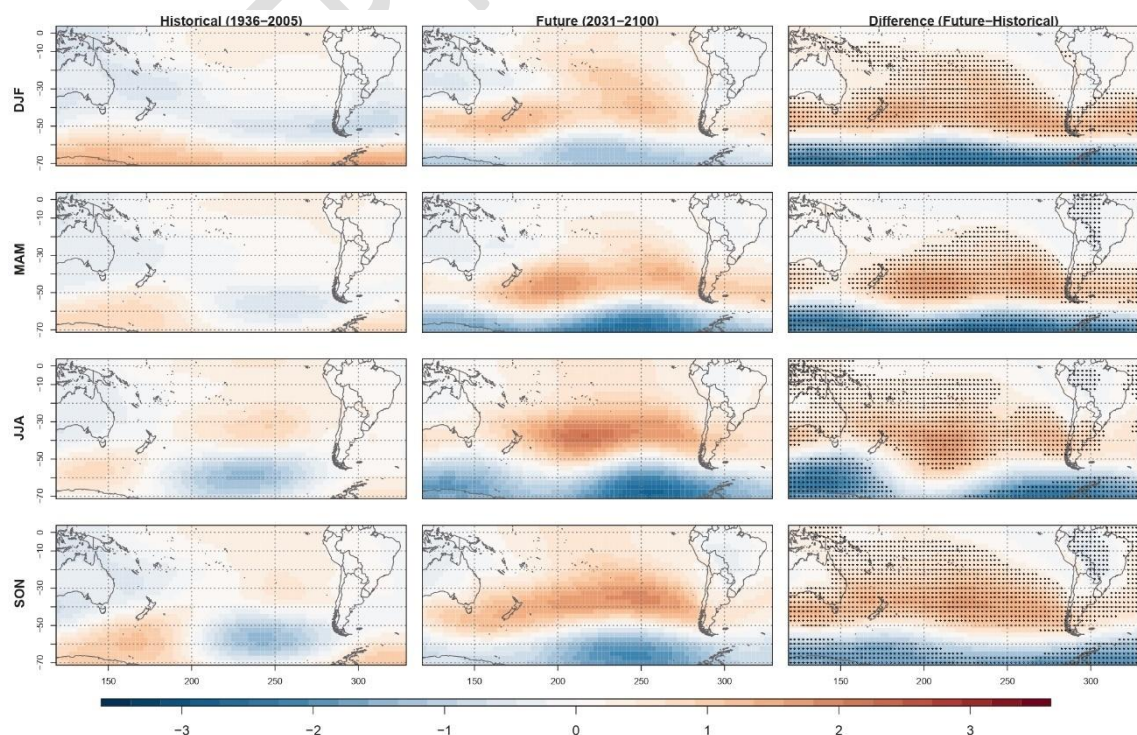


Figure 9: Idem Figure 11 during cold conditions in SST3.4.

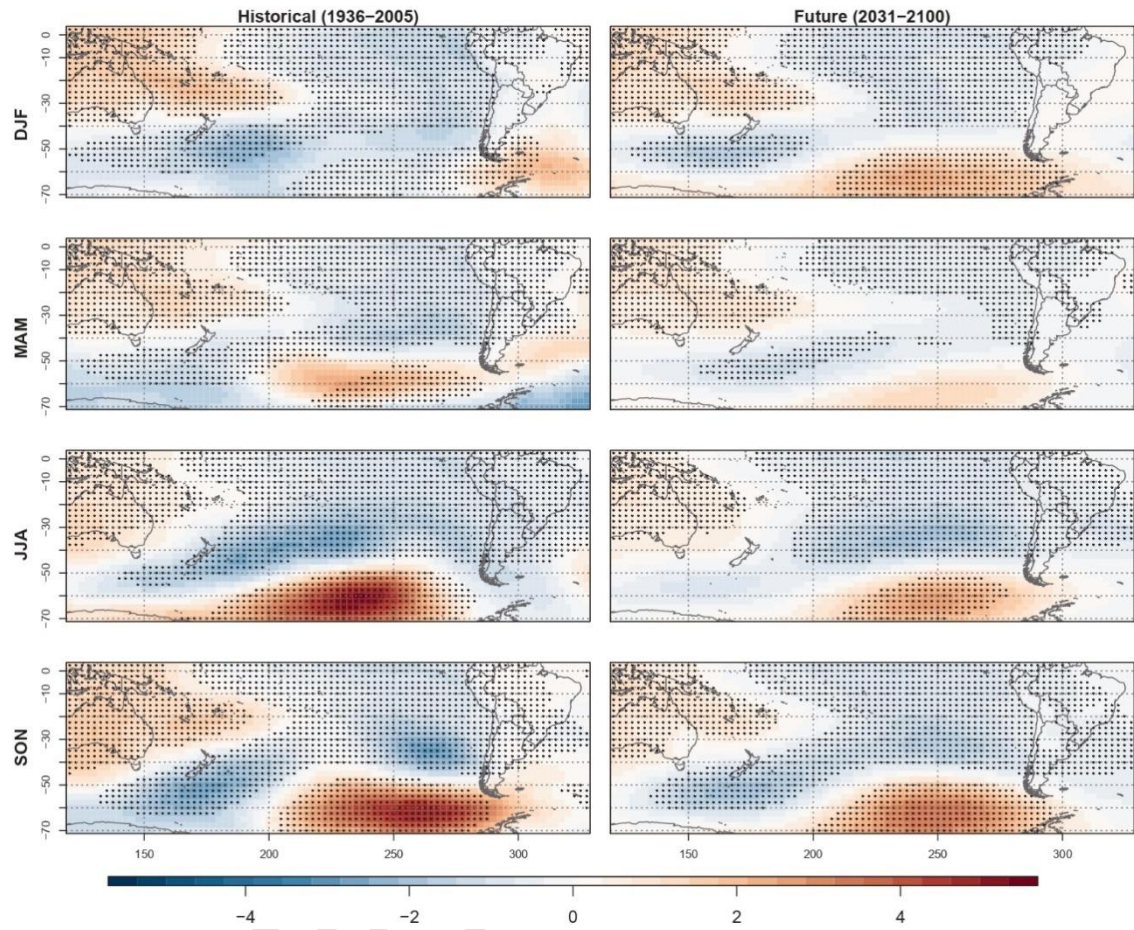


Figure 10: Mean difference of the sea level pressure anomalies [hPa] between El Niño and La Niña events during the historical period (left panel) and the future period (right panel) under the RCP4.5 scenario. Stippling indicates significant differences between El Niño and La Niña at 1%.

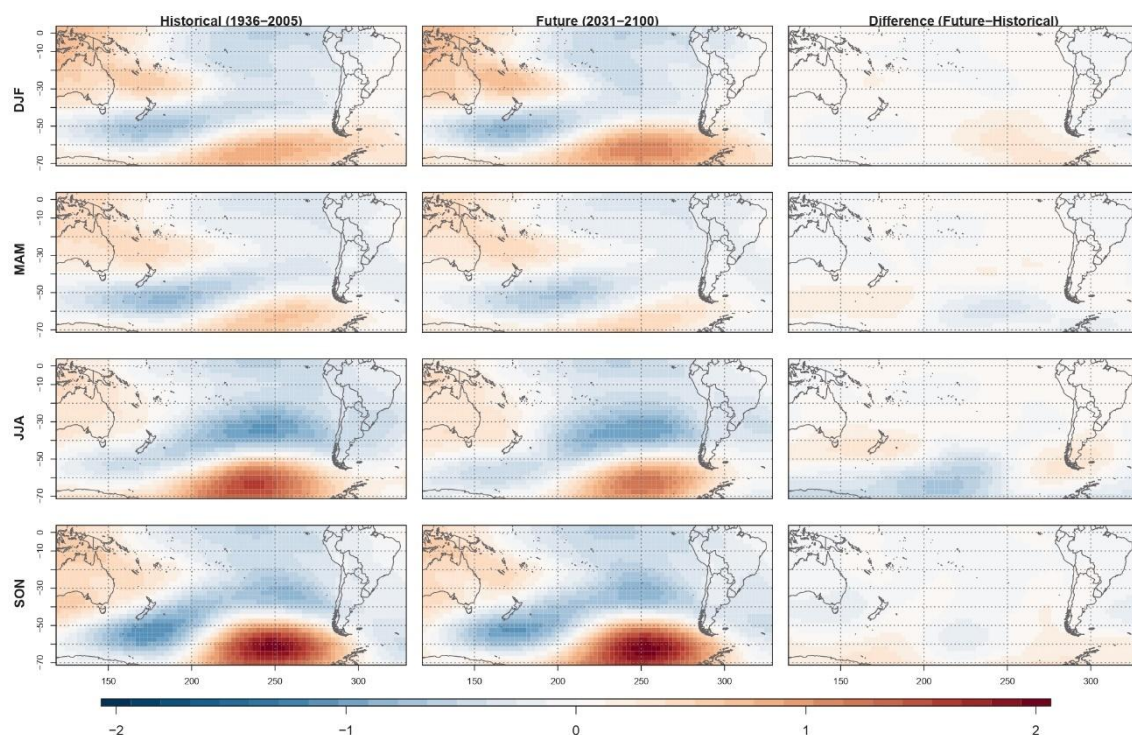


Figure 11: Composites of detrended sea level pressure anomalies [hPa] during warm conditions of the standardized SST3.4 in the historical (1936-2005) and future (2031-2100) periods under RCP4.5 scenario. The differences among those periods are also show. Stippling indicates significant difference at 1%.